

# Nanocomposites-Based Polyolefins as Alternative to Improve Barrier Properties

J. W. C. Carvalho,<sup>1</sup> C. Sarantópoulos,<sup>2</sup> L. H. Innocentini-Mei<sup>1</sup>

<sup>1</sup>Department of Polymer Technology, College of Chemical Engineering, Campinas State University, Campinas SP, Brazil

<sup>2</sup>Packaging Technology Center, Institute of Food Technology, Campinas SP, Brazil

Received 6 April 2009; accepted 15 March 2010

DOI 10.1002/app.32507

Published online 15 July 2010 in Wiley InterScience (www.interscience.wiley.com).

**ABSTRACT:** This work investigates the influence of some ammonium quaternary compounds as coupling agent in polyethylene/clay nanocomposites to improve the performance of polyethylene used as packaging barrier material. The 3 wt % of vermiculite used as a nanofiller was added to linear low-density polyethylene (LLDPE) and to linear low-density polyethylene grafted with maleic anhydride (LLDPE-g-MA). The analysis results revealed that the influence of both the clay exfoliation in a polymer matrix and the coupling agents on the barrier properties were significant. Among the coupling agents

used, cetylpropyldimethylammonium chloride yielded the best result for vermiculite exfoliation. A reduction of up to 18% in the oxygen-permeability coefficient was observed in the nanocomposites with exfoliated vermiculite. The nanocomposite produced with vermiculite did not prove to be efficient as a moisture barrier against according to the analysis performed. © 2010 Wiley Periodicals, Inc. *J Appl Polym Sci* 118: 3695–3700, 2010

**Key words:** barrier; nanocomposites; organoclay; polyethylene (PE)

## INTRODUCTION

The development and diversification of packaging technology is a very important tool in the protection of perishable products against degradation agents. Materials with good oxygen and humidity barrier properties have been thoroughly investigated, mainly in food-protection packaging.

Polyolefins, in general, are used in large scale as packaging around the world, and the linear low-density polyethylene represents one of the members of this family with broad use. Nevertheless polyolefins as a single polymer have not shown ideal performance features as an oxygen and water barrier, essential for longer shelf-life packaging materials.

The use of inorganic fillers dispersed in polymeric matrices, especially phyllosilicates, can be one of the alternatives to improve the mechanical properties and barrier performance for gases and vapors of polymers used for packaging, as already reported in the literature.<sup>1–5</sup>

One of the properties required in packaging materials is optical characteristics. Films used as packaging must have a high transparency level. Thus, the

use of inorganic fillers shows potential if it does not affect the material transparency, and in some cases, it can promote a significant improvement in this property.<sup>6,7</sup>

Nanocomposites films made of polyolefins and nanostructure fillers show great potential as barrier packaging materials, reducing the oxygen-permeability rate at least by 10%, as compared to values obtained for pure resins, while preserving the transparency. The capacity to work as a oxygen and humidity barrier is clearly a function of both the concentration and the type of organoclay used.<sup>8–10</sup> Furthermore, the efficiency of the system to work as a good barrier is directly related to the nanofiller dispersion in the polymeric matrix. If the filler dispersion takes place preferentially as single layers or individual particles, it will promote a significant increase of the obstacles against the permeate gas, yielding a significative improvement in the barrier property.<sup>11,12</sup>

Incomplete dispersion is responsible for the presence of agglomerates or tactoids, with a consequent reduction in the barrier, thermal, and mechanical properties.<sup>12</sup>

Jacquelot et al.<sup>13</sup> confirmed a reduction of approximately 10% in the oxygen-permeability coefficient for LLDPE-g-MA with the addition of 5 wt % nanoclay, proving to be efficient in enhancing the permeated-gas barrier property after its exfoliation. Similar results were found in the study done by Hotta and

Correspondence to: L. H. Innocentini-Mei (lumei@feq.unicamp.br).

**TABLE I**  
Typical Composition of the Vermiculite Supplied

Compound	wt %	Compound	wt %
SiO <sub>2</sub>	40.63	MgO	24.08
Al <sub>2</sub> O <sub>3</sub>	17.58	Fe <sub>2</sub> O <sub>3</sub>	8.38
TiO <sub>2</sub>	0.76	K <sub>2</sub> O	6.61
P <sub>2</sub> O <sub>5</sub>	0.11	CaO	1.35
Na <sub>2</sub> O	<0.10	Cl	<0.10
MnO	<0.10	SO <sub>3</sub>	<0.10
Cr <sub>2</sub> O <sub>3</sub>	<0.10		

Paul<sup>14</sup> showing the improvement of the oxygen barrier property for LLDPE-g-MA and organoclay-compounds films.

As polyolefins are made of hydrocarbon chains, as LLDPE, they are highly hydrophobic and thus act as a good water vapor barrier. However, Dumont et al.<sup>15</sup> reported a four-fold increase in water vapor permeability when using a polyolefin nanocomposite with maleic anhydride containing organoclay. The addition of small amounts of maleic anhydride in the polyolefin matrices is a broadly used strategy to enhance their affinity with the inorganic fillers, improving the compatibility of the polyolefin-based system.

Within the same line, the aim of this study is to prepare chemically modified nanoclays and explore the efficiency of linear low-density polyethylene loaded with these nanoclays to promote the barrier properties of nanocomposites prepared by melt compounding, using as a base resin with and without grafted LLDPE. The results of the barrier property tests focused on the composition and morphological characteristics of the samples prepared with different coupling agents based on ammonium compounds. The samples were investigated with X-ray diffraction (XRD) and scanning transmission electron microscopy (SEM). The effects of the specific interactions between the samples produced with the organically-modified clay and the compounds without clay modification were taken into account in the discussion.

## EXPERIMENTAL

### Materials

Vermiculite was provided by Eucatex Química e Mineral Ltda (São Paulo, SP, Brazil), taken from a mine located in Queimada Nova, Piauí State. A particle size <0.25 mm was selected for this study. Before being used, the vermiculite was dried in an oven at 300 ± 5°C for 24 h to eliminate the water absorbed during the ore washing and used without further purification. The vermiculite composition is presented in Table I.

The organo-vermiculite derivatives were produced with vermiculite and three quaternary salts, such as ammonium chloride, which were used as coupling agents. Table II shows the evaluated compounds. The alkyldimethylbenzylammonium chloride was supplied by Clariant (São Paulo, SP, Brazil), whereas trimethylbenzylammonium chloride and cetylpropyldimethylammonium chloride were provided by Tecmatiz (São Paulo, SP, Brazil) and Capuani (São Paulo, SP, Brazil), respectively.

The polyolefins used, i.e. linear low-density polyethylene [LLDPE, DOWLEX<sup>TM</sup> 2045B, MI = 1.0 g/10 min (2.16 kg @ 190°C), density = 0.920 g/cm<sup>3</sup>], and the linear low-density polyethylene grafted with maleic anhydride [LLDPE-g-MA, AMPLIFY<sup>TM</sup> GR 214, MI = 1.0 g/10 min (2.16 kg @ 190°C), density = 0.922 g/cm<sup>3</sup>, MAH graft level = 0.18 wt %], were provided by Dow Chemical (Midland, MI). The chemical reagents used were analytical grade and were used without any treatment.

### Sample preparation

Sodium vermiculite was prepared from vermiculite in an aqueous solution with 30 wt % sodium chloride. The solution was kept at 60 ± 5°C and stirred continually for 600 h. The solids were filtered and washed with distilled water until the negative reaction for chloride was reached, after which they were dried at 100 ± 5°C for 24 h.

The sodium vermiculite produced was analyzed for its cationic exchanged capacity (CEC),<sup>16,17</sup> resulting in a value of 74.7 ± 1.6 meg/100 g. This value was used as a reference in the organo-vermiculites synthesis. The vermiculite organo derivatives were prepared in a water solution containing sodium vermiculite 5 wt % and ammonium quaternary compounds, using 110% of its CEC value, as show in Table II. The water solution was stirred at 60 ± 3°C for 24 h. The solids were filtered and washed with distilled water at 70 ± 5°C until negative reaction for chloride was reached. The solids were dried in an oven at 80 ± 5°C for 24 h.

The performance of the process was verified through infrared spectroscopy analysis using a Fourier Transformed Infrared spectroscope – FTIR, Thermo Nicolet Nexus 470 (Thermo Fisher Scent., Waltham, MA), with an Automated Total

**TABLE II**  
Ammonium Chloride Compounds Evaluated as Coupling Agents

Compounds
AM-01 - Alkyldimethylbenzylammonium chloride
AM-02 - Trimethylbenzylammonium chloride
AM-07 - Cetylpropyldimethylammonium chloride

**TABLE III**  
**Composition of Nanocomposites Samples and LLDPE**  
**Matrices with and Without Graphitization**  
**Used as References**

Sample	Base resin	Nanofiller
2045 B	LLDPE	–
GR214	LLDPE-g-MA	–
MAPE-BCO	LLDPE-g-MA	Vermiculite
MAPE-AM-01	LLDPE-g-MA	Organo-vermiculite AM-01
MAPE-AM-02	LLDPE-g-MA	Organo-vermiculite AM-02
MAPE-AM-07	LLDPE-g-MA	Organo-vermiculite AM-07

Reflectance – ATR module with a resolution of  $4\text{ cm}^{-1}$  and 32 scans per analysis within the  $4000$  to  $400\text{ cm}^{-1}$  range.

The nanocomposites melt-compounding preparation was performed in a homogenizer from Haake, Polylab 0S/ Rheo Drive 16 model (Thermo Elec., Newington, NH), coupled with a Banbury mixer, Rheomix 05 model, under the following conditions: 60 rpm blade speed,  $180^\circ\text{C}$  processing temperature, and 15 min mixing time. The sample compositions are summarized in Table III. To investigate the effect of the ammonium compounds on the barrier properties, polyethylene and pure vermiculite compounds were used as references.

#### Methods of characterization

The morphological analysis of the nanocomposites was performed through the XRD technique using  $\text{Cu K}\alpha$  as the radiation source. The Rigaku, Dmax 2500 PC model (Rigaku Corp., Tokyo, Japan) equipment was used with graphite monochromator and operated at 40 kV and 150 mA.

The sample sheets for the barrier performance tests, as well as the samples for the structural studies (XRD and SEM), were produced through compression molding in a Carver laboratory press (Carver, Wabash, IN) at  $180^\circ\text{C}$  and 150 bars. The samples sheets thicknesses were determined with a flat micrometer-edge, from Starrett (Starrett Co., Athol, MA) with a resolution of  $1\text{ }\mu\text{m}$ , according to ASTM D 374.

The oxygen-permeability coefficient was determinate through coulometry according to ASTM D 3985 in Oxtran equipment, 2/20 Type, from Mocon (Mocon, Minneapolis, MN), operating with pure oxygen as the permeant gas at  $23^\circ\text{C}$ . The effective permeation area of each sample was of  $50\text{ cm}^2$ . The results were adjusted to 1 atm of the partial oxygen pressure gradient.

The water vapor permeability coefficient was determinate according to ASTM F 1249 in a PERMATRAN unit with an infrared sensor, W3/31 model, from Mocon, (Mocon, Minneapolis, MN). The test was performed at  $38^\circ\text{C}/100\%\text{RH}$  with a of  $5.10\text{ g}$  of

water/ $(\text{m}^2\text{ day})$  calibration standard. The results were adjusted for the  $38^\circ\text{C}/90\%\text{RH}$  condition.

The nanoclay morphology was followed by scanning electron microscopy (SEM) in CEM-902 equipment from Zeiss (Carl Zeiss SMT, MA) operating at 80 kV. For the SEM observation, the samples were prepared with a focused ion beam (FIB) accessory, from FEI (FEI Co., Hillsboro, OR) operated at 30 kV and 50 pA with a gallium ion beam.

## RESULTS AND DISCUSSION

FTIR analysis was used to follow the interactions between the ammonium compounds and the vermiculite during the organo-vermiculite synthesis. Figure 1 shows the organo-vermiculites derivatives FTIR spectra (AM-01, AM-02, and AM-07) and the pure vermiculite, used as references to compare the organo-vermiculite synthesis effectiveness.

In Figure 1, the presence of the characteristic peaks within the  $3000$  to  $2800\text{ cm}^{-1}$  range that appears in all of the compounds where the interaction of vermiculite and the ammonium compound occurred was observed. These peaks represent the stretching vibrations of symmetrical and asymmetrical  $\text{CH}_2$ , presented in the  $\text{CH}_2$  and  $\text{CH}_3$  of the quaternary ammonium coupled to the vermiculite, further confirming the presence of organo-vermiculite derivatives.

These results are supported by those obtained in the study performed by Araújo et al.<sup>18</sup> and Xu et al.<sup>19</sup> with similar coupling agents.

Figure 2 shows the MAPE serie compounds' XRD spectra produced with LLDPE-g-MA and the organo-vermiculites AM-01, AM-02, and AM-07, and the spectrum produced with the same base resin

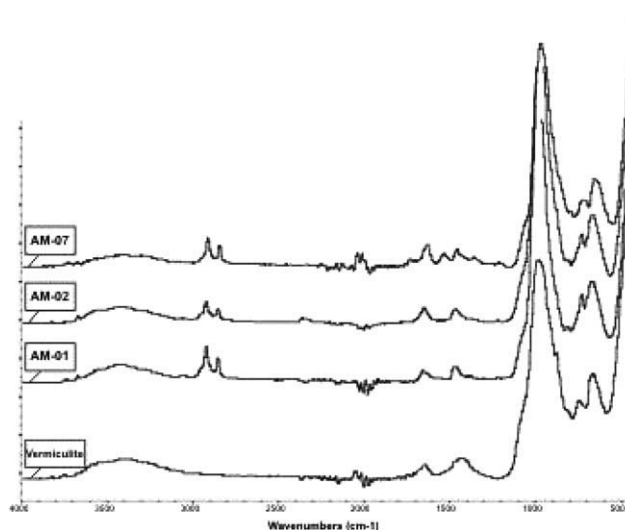


**Figure 1** FTIR vermiculite spectra (below) in comparison to organo-vermiculites spectra, synthesized with ammonium compounds and vermiculite.

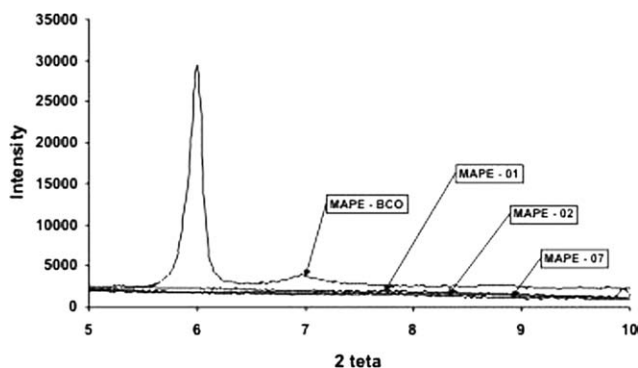


**Figure 2** XRD spectrum of nanocomposite with organo-vermiculites, compared to the compound with pure vermiculite (MAPE-BCO).

and pure vermiculite (MAPE-BCO). It is known from the literature<sup>20</sup> that based on the position of the peak located at  $2\theta = 7.3^\circ$ , it is possible to analyze the thickness of the vermiculite layers. Thus, the absence of this peak implies that the vermiculite-layers thickness value is beyond the equipment detection limit. This ensures that the vermiculite exfoliation has occurred in the analyzed compound. Figure 2 also shows that the MAPE-BCO sample did not show the exfoliation, as it is possible to observe the presence of a peak at  $2\theta = 7.3^\circ$ . Using the MAPE-BCO-sample spectrum in Figure 2 as a reference, it is possible to assume that the others MAPE compounds (MAPE-01, MAPE-02, MAPE-07) present these exfoliated structures due the absence of the at  $2\theta = 7.3^\circ$  peak.

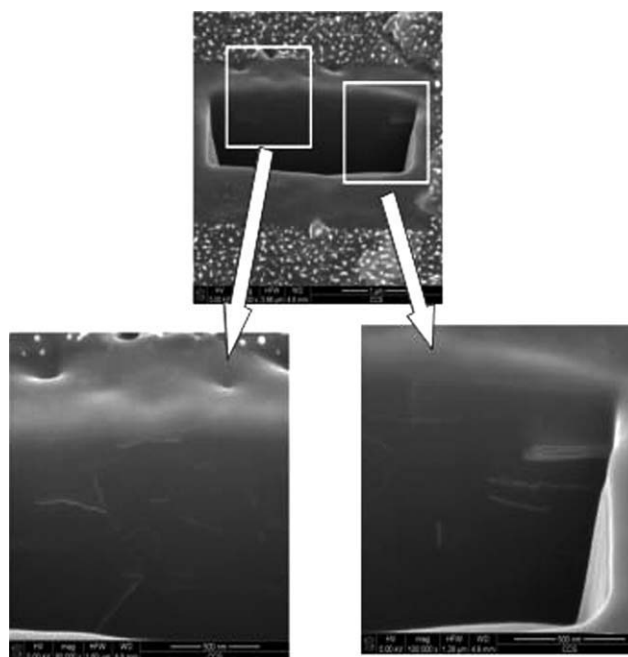
To ensure the nanocomposite formation, the samples were analyzed through SEM using the FIB procedure. Figure 3 shows the image obtained for the MAPE AM-07 nanocomposite sample and the details of the material bulk structure.

As seen in the polymeric matrix in Figure 3, some vermiculite layers appear dispersed in the bulk of the matrix, which characterizes the occurrence of exfoliation, thus confirming the nanocompound production.

### Gas permeability

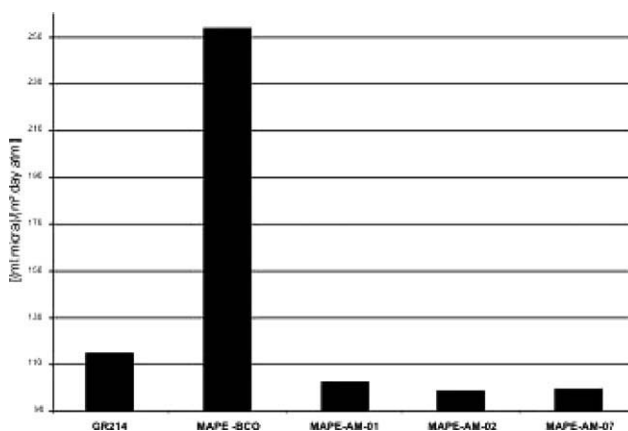
The MAPE serie compounds were tested as oxygen- and water vapor barriers. Figure 4 shows the results for the oxygen-permeability coefficient of the compounds produced with the coupling agents compared to the LLDPE-g-MA base resin with pure vermiculite (MAPE-BCO) and without vermiculite (GR214).

Figure 4 shows the oxygen leak measurements for various systems, indicating a significant reduction in the oxygen flow, as observed for those compounds produced with organo-vermiculite.



**Figure 3** SEM microphotographs showing the MAPE-AM-07 sample prepared through the FIB procure, showing the formation of this nanocompound.

The effect of the ammonium compound absence in the permeability coefficient can be observed for the MAPE-BCO sample produced with LLDPE-g-MA and pure vermiculite. This compound presents a very high value in the oxygen permeability, as observed in Figure 4, suggesting that the vermiculite works only as a simple mineral filler with no interaction with the polymeric matrix. Such behavior implies that the compound is not exfoliated like the others, as confirmed by XRD analyses shown in Figure 2. This result was already expected due to the incompatibility of pure vermiculite with the polymer matrix, avoiding the compound exfoliation. Consequently, channels are formed through the compound



**Figure 4** Permeability coefficient for oxygen in the MAPE series compared to the base resins with pure vermiculite (MAPE-BCO) and without vermiculite (GR214).

**TABLE IV**  
Effect of the Ammonium Compounds in Oxygen Permeability in Nanocomposites Compared to Base Resin

	Permeability coefficient (ml $\mu\text{m}$ )/ ( $\text{m}^2 \text{ day atm}$ )	Performance Improvement (%)
GR-214 <sup>(1)</sup>	114.51 $\pm$ 7.23	–
MAPE-AM-01	102.50 $\pm$ 4.01	10.48
MAPE-AM-02	98.28 $\pm$ 5.58	14.17
MAPE-AM-07	93.90 $\pm$ 9.94	18.00

structure, increasing the oxygen permeability as shown in Figure 4 for MAPE-BCO.

From a different point of view, it is possible to associate the permeability increase with the presence of the anhydrides branches, which can increase the spacing between the vermiculite and the polymer-matrix chains, creating preferential channels for the gas flow. This hypothesis was also supported in the literature by the study developed by Zhong et al.<sup>20</sup>

The low oxygen-permeability values observed in the compounds produced with the AM-01, AM-02, and AM-07 organo-vermiculites could be associated with the presence of ammonium compounds. These improve the capacity of the inorganic phase dispersion due to the ammonium compound compatibility, which acts at on the nanofiller/polymer interface. This inorganic phase represented by the vermiculite increases the gas flow barriers in the compound, thereby reducing the oxygen permeability. Note that the presence of the ammonium compounds in the nanocomposites showed a significant reduction in the oxygen permeability of up to 18%, as shown in Table IV. This result is further confirmed by the study performed by Bagrodia et al.,<sup>12</sup> who reported a reduction of at least 10% in the oxygen permeability and its dependence on the organo-silicate concentration used.

The effectiveness of the oxygen barrier with the reduction of permeability is directly proportional to the dispersion of inorganic material in the polymeric matrix. A good dispersion, which leads to the nanofiller exfoliation, will promote a more tortuous path for the gas flow. This concept is presented in the literature by several authors based on the average free path increase principle.<sup>14,20,21</sup>

The dispersion and exfoliation process are synergistically supported by the ammonium quaternary compounds, which helps enhance the polymer-matrix interaction during the phyllosilicate galleries interposing. This behavior can be observed in Table IV, where the differences between the oxygen permeation results are the result of the various quaternary ammonium compounds actions used in the vermiculite dispersion. In the analysis of the results presented in Table IV it is possible to observe the

good performance of the cetylpropyldimethylammonium chloride as the MAPE-AM-07 nanocomposite coupling agent that presents the best result for the oxygen-permeability coefficient.

The AM-07 ammonium compound has a spatial structure with a bulk radical that contributes to the formation of most spaced organo-vermiculite layers. These spaces between the layers are created during the organo-vermiculite synthesis process, and during the hot melt interposing they were easily filled with LLDPE-g-AM, resulting in vermiculite exfoliation and giving rise to the MAPE-AM-07 nanocomposite.

Note that the permeability reduction with the use of the AM-07 amine was superior to those structures containing benzyl radicals presented in the AM-01 and AM-02 compounds. When the radical size is analyzed, there is an important factor in the phyllosilicates layers thickness increase. Good permeability reduction results were also obtained in samples with AM-01 and AM-02, but the reduction was lower than that achieved by the compound prepared with AM-07.

The analysis of the results of the organo-vermiculite with a coupling agent for the cetylpropyldimethylammonium chloride and the polymer matrix composed of LLDPE-g-MA strongly suggests the use of these nanocomposites for packaging where the oxygen barrier is the most important parameter to be considered.

Figure 5 compares the water vapor permeability results presented as a coefficient of permeability in the MAPE series compared to the base resin (GR214) and pure vermiculite (MAPE-BCO).

Figure 5 shows that the hydrophobic matrix made with LLDPE-g-MA increases its water vapor barrier property when it is blended with hydrophilic particles, regardless of the coupling agent used. This behavior can be explained by the affinity of the water molecules with the vermiculite surface. The

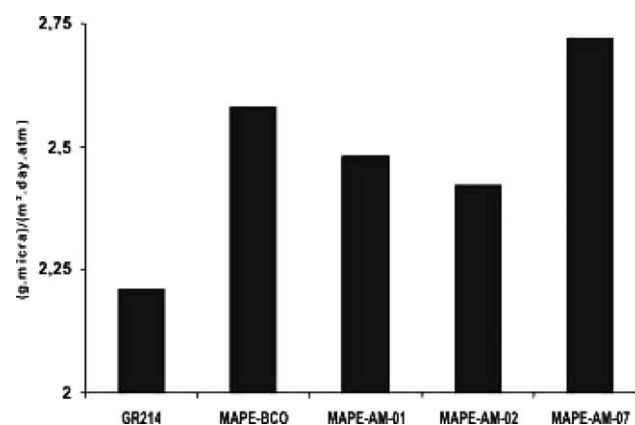


**Figure 5** Water vapor permeability coefficient in MAPE samples compared to base resin and pure vermiculite compounds.

localized absorption points for the formation of preferential channels in the polymeric matrix in the region between neighboring inorganic particles results in an increase of the nanocomposite water permeability. The channel formation and its water permeability increase in nanocomposites are supported by Dumont et al.<sup>15</sup>

In general, an increase from 9.5 to 23.0% in the water vapor permeability value in all of the samples analyzed when compared to base resin can be observed. Similar results were reported by Hotta and Paul<sup>14</sup> using analogous compounds as samples in their study.

### CONCLUSIONS

The results obtained clearly show that it is possible to produce nanostructured composites directly from pure vermiculite, showing a very interesting and economical alternative for packaging material where the main drive is the oxygen barrier. The obtainment of sodium vermiculite is the first step to produce organo-vermiculite, and finally its nanocomposites using the PEBDL-*g*-AM as the polymeric matrix, through hot melt intercalation.

The coupling agents' influence on the produced nanocomposites barrier properties was evidenced by the significant reduction of up to 18% in the oxygen-permeability coefficient, using 3 wt % of phyllosilicates added as vermiculite.

Among the coupling agents used, cetylpropyldimethylammonium chloride presents the best result in the vermiculite exfoliation process, and thus yielded the best performance in reducing the oxygen permeability in nanocomposites produced.

The nanocomposites obtained were not effective in improving the water barrier due the vermiculite characteristic of adsorbing humidity and creating preferential channels for water vapor.

The XRD and SEM techniques with FIB were very helpful in detecting the presence of nanofiller exfoli-

ation and dispersion in the polymeric matrix, whereas FTIR was useful to confirm the vermiculite chemical modification.

Thanks are due to Dr. Edson Leite, Dr. Yimsan Gau, and Dr. André Giraldi, for their valuable collaboration.

### References

1. Beall, G. W.; Tsipursky, S.; Sorokim, A.; Goldman, A. U.S. Pat. 5,880,197 (1999).
2. Frisk, P. U.S. Pat. 5,916,685 (1999).
3. Barbee, R. B.; Matayabas, J. C.; Trexler, J. W.; Piner, R. L.; Gilmer, J. W.; Connell, G. W.; Owens, J. T.; Turner, S. R. U.S. Pat. 6,713,547 (2004).
4. Akkapeddi, M. K.; Socci, E. P.; Kraft, T. J. U.S. Pat. 6,756,444 (2004).
5. Wang, Y.; Hsieh, T.-E. *Chem Mat* 2005, 17, 3331.
6. Knoll, R.; Mueller, C. U.S. Pat. 6,841,211 (2005).
7. Maruyama, T.; Ishikawa, K.; Amino, N.; Ikawa, M. U.S. Pat. 6,908,958 (2005).
8. Arunvisut, S.; Phummanee, S.; Somwangthanaroj, A. *J Appl Polym Sci* 2007, 106, 2210.
9. Osman, M. A.; Mittal, V.; Suter, U. W. *Macromol Chem Phys* 2007, 208, 68.
10. Yano, K.; Usuki, A.; Okada, A. *J Polym Sci Part A: Polym Chem* 1997, 35, 2289.
11. Sakaya, T.; Kuroda, R.; Ogawa, T. U.S. Pat. 5,854,326 (1998).
12. Bagrodia, S.; Germinario, L. T.; Gilmer, J. W.; Lan, T.; Psihogios, V. U.S. Pat. 6,586,500 (2003).
13. Jacquelot, E.; Espuche, E.; Gerard, J.-F.; Duchet, J.; Mazabraud, P. *J Polym Sci Part B: Polym Phys* 2006, 44, 431.
14. Hotta, S.; Paul, D. R. *Polymer* 2004, 45, 7639.
15. Dumont, M.-J.; Reyna-Valencia, A.; Emond, J.-P.; Bousmina, M. *J Appl Polym Sci* 2007, 103, 618.
16. Dal Bosco, S. M.; Jimenez, R. S.; Carvalho, W. A. *J Colloid Interface Sci* 2005, 281, 424.
17. A.O.A.C. Method 979-09; Association of Official Analytical Chemists, 15th ed.; Association of Official analytical Chemists: Washington D.C., USA, 1990.
18. Araújo, E. M.; Melo, T. J. A.; Oliveira, A. D.; Araújo, H. L. D.; Araújo, K. D.; Barbosa, R. *Polímeros* 2006, 16, 38.
19. Xu, J.; Li, R. K. Y.; Xu, Y.; Li, L.; Meng, Y. Z. *Eur Polym J* 2005, 41, 881.
20. Zhong, Y.; James, D.; Zheng, Y.; Hetzer, M.; De Kee, D. *J Polym Eng Sci* 2007, 47, 1101.
21. Brulé, B.; Flat, J. J. *Macromol Symp* 2006, 23, 210.